Separation Science and Technology
Publication details, including instructions for authors and subscription information:
http://www.informaworld.com/smpp/title~content=t713708471

Gel Permeation Chromatography Calibration. I. Use of Calibration Curves Based on Polystyrene in THF and Integral Distribution Curves of Elution Volume to Generate Calibration Curves for Polymers in 2,2,2-Trifluoroethanol

Theodore Provder[ab]; James C. Woodbrey[a]; James H. Clark[a]
[a] MONSANTO COMPANY ST. LOUIS, MISSOURI [b] Glidden-Durkee Division, Dwight P. Joyce Research Center, SCM Corporation, Strongsville, Ohio

To cite this Article Provder, Theodore , Woodbrey, James C. and Clark, James H.(1971) 'Gel Permeation Chromatography Calibration. I. Use of Calibration Curves Based on Polystyrene in THF and Integral Distribution Curves of Elution Volume to Generate Calibration Curves for Polymers in 2,2,2-Trifluoroethanol', Separation Science and Technology, 6: 1, 101 — 136
To link to this Article: DOI: 10.1080/00372367108055554
URL: http://dx.doi.org/10.1080/00372367108055554

SEPARATION SCIENCE, 6(1), pp. 101–136, February, 1971

Gel Permeation Chromatography Calibration. I. Use of Calibration Curves Based on Polystyrene in THF and Integral Distribution Curves of Elution Volume to Generate Calibration Curves for Polymers in 2,2,2-Trifluoroethanol*

THEODORE PROVDER,† JAMES C. WOODBREY, and JAMES H. CLARK

MONSANTO COMPANY
ST. LOUIS, MISSOURI 63166

Summary

A general method is proposed for obtaining gel permeation chromatographic (GPC) molecular weight (MW) and hydrodynamic volume (HDV) calibration curves for polymer–solvent systems where primary polymer standards are unavailable. The method is demonstrated by using a HDV calibration curve based on polystyrene in tetrahydrofuran (THF), in conjunction with integral distribution curves of elution volume for poly(methyl methacrylate) (PMMA) in THF and in 2,2,2-trifluoroethanol (TFE) for the generation of a HDV calibration curve in TFE. Transformation methods for generating secondary MW calibration curves from HDV calibration curves are discussed and applied to PMMA in THF and TFE, and to poly(trimethylene oxide), poly(vinyl acetate), and certain polyamides in TFE. The utility and reliability of the secondary calibration curves are demonstrated by comparing MW

* Presented at the ACS Symposium on Gel Permeation Chromatography sponsored by the Division of Cellulose, Wood and Fiber Chemistry at the 159th National Meeting of the American Chemical Society, Houston, Texas, February 1970.

† Present address: Dwight P. Joyce Research Center, Glidden-Durkee Division, SCM Corporation, 16551 Sprague Road, Strongsville, Ohio 44136.

averages and intrinsic viscosities obtained by GPC and by the classical methods. Molecular structural differences among the polyamide samples associated with the distribution of short- and long-chain branches are discussed in relation to their secondary calibration curves.

INTRODUCTION

The solvent most commonly used for the gel permeation chromatography (GPC) characterization of polyamides has been *m*-cresol. The solvent 2,2,2-trifluoroethanol (TFE) also is a good solvent for polyamides and has many more desirable properties than *m*-cresol. The differential refractive index of poly(methyl methacrylate) (PMMA) and polyamide polymers is greater in TFE than in *m*-cresol. In order to obtain the equivalent recorder response at a sensitivity of 4× for a refractometer with a 0.004-in. slit, polymer concentrations >0.3 w/v-% must be used in *m*-cresol compared to concentrations <0.1 w/v-% in TFE. The high concentrations that must be used in *m*-cresol can cause column overloading and increase chromatogram peak spreading due to dispersion, skewing, and flattening effects (*1, 2*). The higher operating temperature, >100°C, required for the highly viscous *m*-cresol, compared to the 50°C operating temperature for TFE, has been shown to lead to polymer degradation (*3, 5*). TFE does not degrade polyamides at 50°C. *m*-Cresol is subject to oxidative degradation and has additional annoying low-molecular-weight impurity peaks (*4*) which contribute to baseline instability and interfere with the normal chromatogram. TFE has only the normal air and water peaks. The water peak in TFE is controllable by solvent and sample drying techniques to be discussed later. Unlike *m*-cresol, TFE does not burn the skin and is less toxic than tetrahydrofuran (THF). However, with all these advantages, the one main disadvantage connected with using TFE as a GPC solvent is the insolubility of the readily available characterized anionic polystyrene (PS) standards. This insolubility prevents the generation of primary and secondary calibration curves in TFE.

In this paper a method will be presented that removes this difficulty. This method makes use of the hydrodynamic volume (HDV) calibration curve in THF constructed from PS standards, and integral distribution curves of elution volume in THF and TFE for uncharacterized PMMA samples, for the generation of a HDV calibration curve in TFE. Two methods will be presented for the construction of molecular weight calibration curves from a HDV calibration curve.

These methods will be applied to PMMA in THF and PMMA, poly-(vinylacetate) (PVAC), certain polyamides, and poly(trimethylene oxide) (PTMO) in TFE.

MATERIALS AND METHODS

Samples

Fourteen PMMA samples were prepared by routine free-radical bulk and solution polymerization methods (*6*). These samples covered a wide molecular weight range. A blend of these samples was fractionated on a Waters Associates Ana-prep GPC in THF with a Styragel column having a nominal porosity of 10^4 Å. Seven useful fractions were obtained and denoted as C, D, F, G, H, I, and J. The baseline-adjusted elution volume curves of these fractions in TFE are shown in Fig. 1. The conditions under which these and other GPC

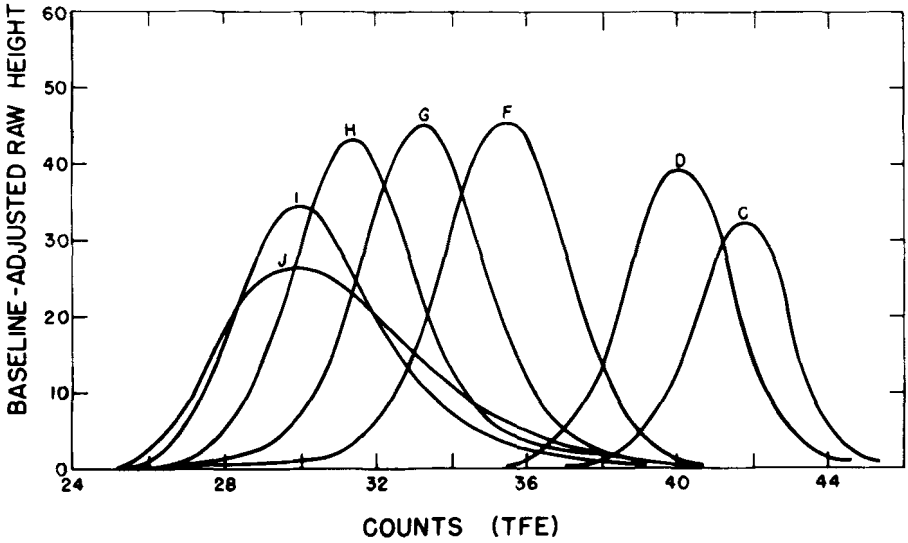

FIG. 1. Baseline-adjusted chromatograms of PMMA Fractions C, D, F, G, H, I, and J.

curves were obtained are described later in this paper. A more detailed report describing the preparation and Ana-prep fractionation of the PMMA blend, and molecular structure characterization of the resulting fractions will be published later (*7*).

Anionically polymerized caprolactam samples were prepared according to methods described by Gechele and Stea (*8*), and by Greenley, Stauffer, and Kurz (*9*). The synthesis conditions of these experimental polycaprolactam (PC) samples, which are designated as PC-4, PC-5, PC-6, PC-7, and PC-8, are shown in Table 1. Fractions

TABLE 1

Synthesis Conditions of Experimental Polycaprolactam Samples

Sample designation	Catalyst (concn)[a]	Initiator (concn)[b]	Polymerization temp. (°C)
PC-4	NaH (1/100)	N-AcCL[c] (1/100)	160
PC-5	EtMgBr (1/200)	N-AcCL (1/100)	130
PC-6	EtMgBr (1/796)	N-AcCL (1/398)	140
PC-7	NaH (1/600)	N-AcCL (1/600)	160
PC-8	NaH (1/67)	Is-A[d] (1/200)	160

[a] Number of moles of catalyst per mole of monomer.
[b] Number of moles of initiator per mole of monomer.
[c] N-Acetylcaprolactam.
[d] Isatoic anhydride.

of some of these PC samples were obtained by separate use of sand-column-elution fractionation and coacervation fractionation techniques with *m*-cresol–cyclohexane mixtures. Fractions obtained from the sand-column-elution fractionation are designated by symbols F3, F4, F5, etc., which indicate 1st, 2nd, 3rd, etc., fractions, respectively. Generally, the molecular weight increases with increasing fraction number. Fractions obtained from the coacervation fractionation are designated by the symbols P1, P2, P3, etc., which indicate 1st, 2nd, 3rd, etc., fractions, respectively. Generally, the molecular weight decreases with increasing fraction number. When a P2 fraction was fractionated further by sand-column-elution fractionation, the fractions were denoted as F1P2, F2P2, F3P2, etc. A detailed report describing the fractionation and characterization of these PC samples will be published later (*10*). The baseline-adjusted elution volume GPC curves of the PC samples and fractions used in this study are shown in Figs. 2–5.

A commercial PC sample made by hydrolytic polymerization methods was obtained from Allied Chemical Corporation and is designated as P-8205. A commercial sample of PVAC was obtained from Farbwerke Hoechst A.G. through Prof. H. Benoit as part of the

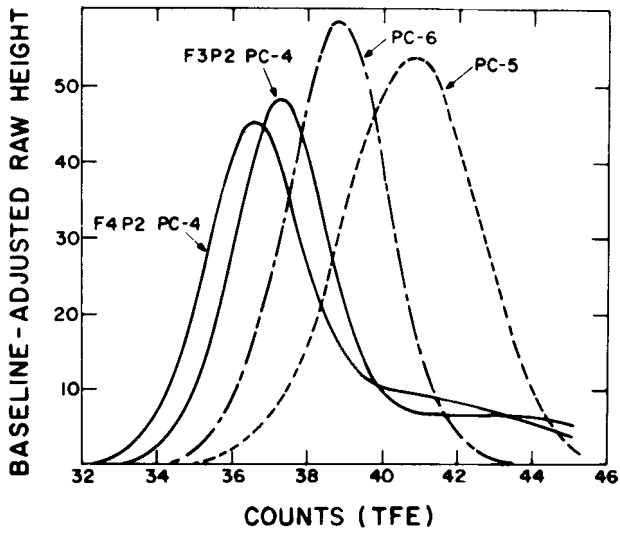

FIG. 2. Baseline-adjusted chromatograms of Samples F3P2 PC-4, F4P2 PC-4, PC-5, and PC-6.

IUPAC polymer study program. An experimental sample of PTMO made by cationic polymerization methods was provided by Dr. R. E. Wetton of the University of Technology, Loughborough, Leicestershire, England. The baseline-adjusted elution volume GPC curves of

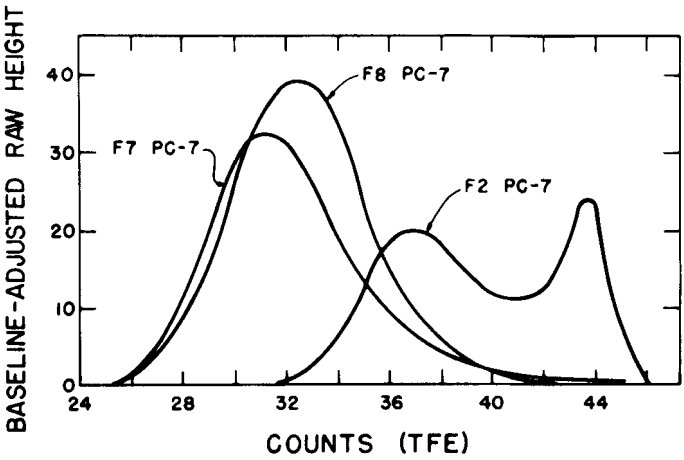

FIG. 3. Baseline-adjusted chromatograms of PC-7 Fractions F2, F7, and F8.

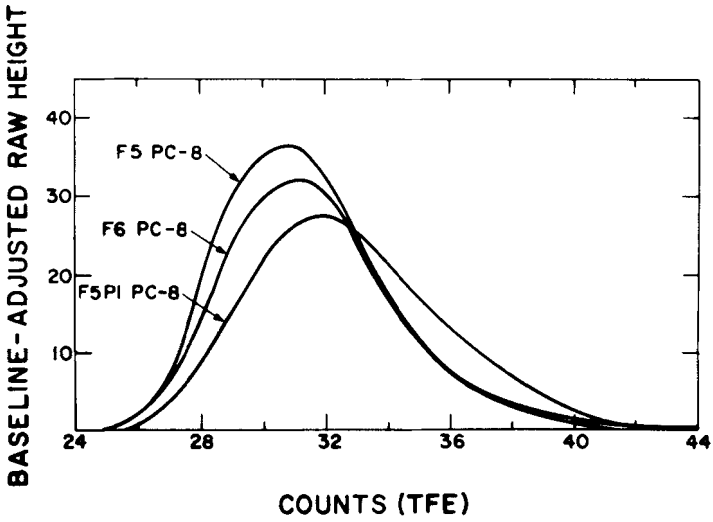

FIG. 4. Baseline-adjusted chromatograms of PC-8. Fractions F5P1, F5, and F6.

the samples P-8205, PVAC, and PTMO used in this study are shown in Fig. 5.

Solvents

Certified reagent grade THF ($n_D^{25} = 0.888$, bp = 64–66°C) obtained from Fisher Scientific Co. was used for both viscometry and GPC. The solvent contained 0.025 (w/v) % di-tertiary-butyl-*p*-cresol which served as an antioxidant. The solvent TFE ($n_D^{20} = 1.2907$, $d^{25} = 1.3823$, bp = 73.6°C, ionization constant $K_a = 4.3 \times 10^{-13}$) was obtained from Halocarbon Products Corp. in Hackensack, N. J. The GPC eluted polymer-contaminated TFE was routinely recovered by first running the solution through a 3-Å molecular sieve column to remove small amounts of water and then fractionally distilling the dried solution. Gas chromatography analysis indicated that the total impurities in the freshly distilled dry solvent were usually less than 0.1%.

Gel Permeation Chromatography

Two Waters Associates Model 200 Gel Permeation Chromatographs, each fitted with five Styragel columns, were used for the analysis of

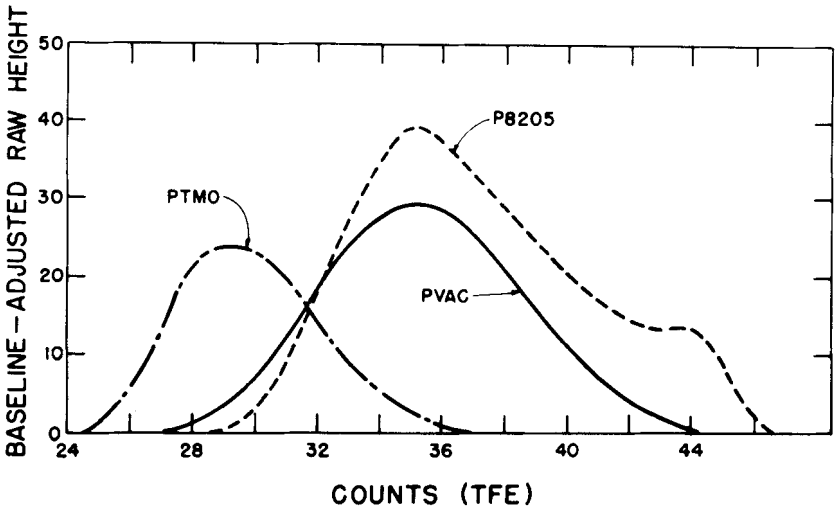

FIG. 5. Baseline-adjusted chromatograms of Samples PVAC, P8205, and PTMO.

molecular weight distributions in THF and TFE. The nominal porosity designations of the column sets used in THF and TFE were 10^6, 10^5, 10^4, 10^3, 250 Å and 10^7, 10^7, 10^6, 1.5×10^5, 1.5×10^4 Å, respectively. The column set used with THF was operated at room temperature, 24 ± 1°C, and had a plate count of 734 plates/foot with *o*-dichlorobenzene, while the column set used with TFE was operated at 50.0 ± 0.5°C and had a plate count of 568 plates/foot with ε-caprolactam. The differential refractometer of the instrument used with THF had a 0.019-in. slit, was operated at a sensitivity of $8\times(100)$, and monitored the effluent streams at 42°C. The degasser was operated at 55°C. The differential refractometer of the instrument used with TFE had a 0.004-in. slit, was operated at a sensitivity of $4\times(100)$, and monitored the effluent streams at 54°C. The degasser was operated at 65°C. The solvent flow rates were controlled at better than 1.00 ± 0.05 ml/min. To eliminate errors in elution volume measurement due to variations in the rate of solvent evaporation in the siphon tube (1 count = 5.024 ml for THF, 1 count = 5.148 ml for TFE), a vapor feedback loop device similar to that of Yau, Suchan, and Malone (*11*) was installed. Polymer samples were dried *in vacuo* overnight at 60°C, dissolved in degassed solvent taken from the GPC solvent reservoir, and then were Millipore-filtered under N_2 pressure

through 0.2 μ Metricel Alpha-8 filters. The polymer samples and PS-calibration standards were injected for 120 sec by means of the Waters Associates Automatic Sample Injection System. All the polymer sample solutions had concentrations <0.1 (w/v) %. The GPC traces were recorded digitally at 20 sec intervals by means of the Waters Associates Digital Curve Translator. Molecular weight averages, intrinsic viscosity, and integral and differential distribution curves were calculated on an IBM 360/65 computer according to the basic integral formulas given by Pickett, Cantow, and Johnson (*12*). These formulas are given later in the paper as Eqs. (7) through (10).

Calibration Standards

The calibration standards used in the construction of the HDV calibration in THF were linear polystyrene standards obtained from Pressure Chemical Co. and Waters Associates. The absolute number- and weight-average molecular weights, polydispersity ratios, and peak elution volume values, designated respectively by $\bar{M}_n(t)$, $\bar{M}_w(t)$, $P(t)$, and PEV, of the PS standards for the column set used with THF were shown in Table 1 of Ref. *1*. The Mark-Houwink intrinsic viscosity-molecular weight relation used to obtain the absolute intrinsic viscosity, $[\eta](t)$, for PS is given by (*1, 13*)

$$[\eta]^{PS}_{THF,25°C} = 1.60 \times 10^{-4} \bar{M}_v^{0.706}, \qquad \bar{M}_v > 3000 \tag{1}$$

The HDV calibration curve obtained from the $[\eta](t)$–$\bar{M}_w$–PEV data for polystyrene in THF is shown in Fig. 6.

Membrane Osmometry

Number-average molecular weights were determined with a Mechrolab Model 501 high-speed membrane osmometer fitted with a Hewlett-Packard variable-temperature controller and 10 mV Texas Instrument Servoriter-II recorder. The PMMA polymers were measured in toluene at 60°C and the PC, PVAC, and PTMO polymers were measured in *o*-chlorophenol (OCP) at 60°C. Schleicher and Schuell, Inc., type 08 deacetylated acetyl cellulose membranes were used for both solvents and were conditioned by the recommended method (*14*) of gradually changing the medium from water through ethanol to the desired solvent. Stable readings were usually obtained with each solvent within 5 min and $\bar{M}_n$ values as low as 5,000 and

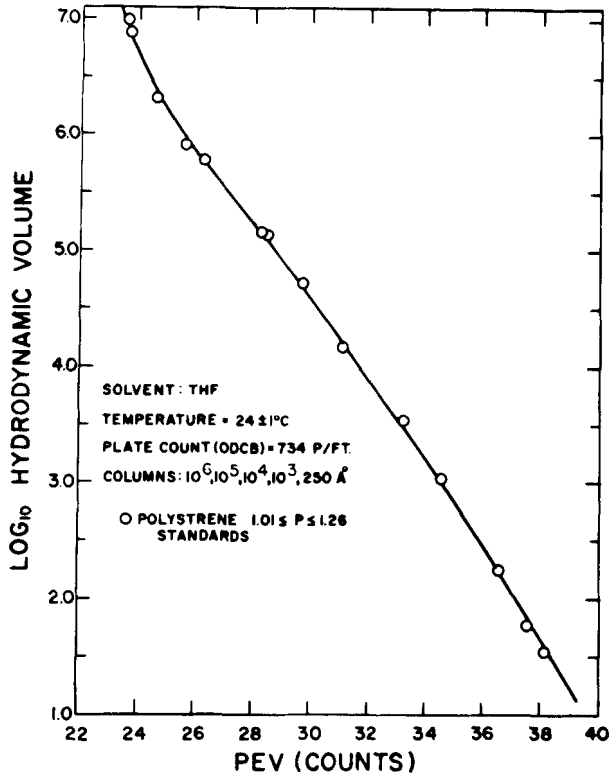

FIG. 6. Polystyrene hydrodynamic volume calibration curve in THF.

15,000 could be determined on polymer fractions in OCP and toluene, respectively, without evidence of diffusion. The membrane life in toluene was 2 weeks, while in OCP it was 4 weeks. The number-average molecular weight was obtained from the intercept (*15*) of a linear least-square fit of five to six values of $\{C, \sqrt{\pi}/C\}$ where π (g/cm^2) is the osmotic pressure and C (g/ml) is the concentration and abscissa of the parameter set. In most cases, the experimental error in $\bar{M}_n$ was less than $\pm 3\%$.

Viscometry

Viscometry measurements were made in THF at 25°C and in TFE at 50°C with uncalibrated Cannon-Ubbelohde dilution viscometers which gave solvent times greater than 100 sec. The viscometers used had centistoke ranges denoted by viscometer sizes of 50 and 75 for THF and TFE, respectively. The solvent and solution efflux times

were determined by means of the Hewlett-Packard Autoviscometer system which includes the Model 5901B Autoviscometer, the Model 5903A Programmer-Printer, and the Model 5910A constant temperature bath. Temperature control was maintained to within ±0.01°C for the temperatures of measurement. Efflux times were measured to ±0.01 sec by means of a photodetector system which consisted of an upper and lower photocell unit that detected meniscus movement. A drying tube containing activated 3 Å molecular sieves was placed between the external air pump and the autoviscometer to eliminate water absorption by the THF and TFE solvents.

Polymer concentrations were chosen such that the highest concentration had an efflux time between 200 and 300 sec. Six solution concentrations were made up volumetrically from a stock solution on a g solute/100 g solution basis and converted to g/dl via the solvent density at the temperature of measurement. The solvent densities used were $d_{TFE}^{50°C} = 1.3429$ obtained from pycnometric measurements (*16*) and $d_{THF}^{25°C} = 0.8811$ (*17*). In order to produce dust-free solutions, the stock solution and solvent were first drawn through a coarse fritted glass disk filter into the pipet before being delivered to the viscometer. Solution efflux times generally had an average deviation of ±0.02 sec. All efflux times were of sufficient duration to justify neglect of kinetic energy corrections.

The intrinsic viscosity, $[\eta]$, was determined from an equivalent form of the Schulz-Blaschke equation (*18*) derived by Heller (*19*) and Ibrahim (*20*). The intrinsic viscosity was the reciprocal of the intercept obtained from a linear-least square fit of $\{C, \eta_{sp}/C\}$ where η_{sp} is the specific viscosity and C (g/dl) is the concentration and the abscissa of the parameter set. In most cases the experimental error in $[\eta]$ was less than ±0.5%.

Light Scattering

The weight-average molecular weights of some of the polycaprolactam polymer fractions were determined from light-scattering measurements carried out with a S.O.F.I.C.A. light-scattering photometer. Measurements were made at room temperature in TFE with unpolarized light of 546 mμ wavelength. Solutions were filtered by gravity through Metricel Alpha-8 0.2 μ filters directly into the measuring cell in order to produce dust free solutions. The instrument was calibrated with benzene (*21*). The average specific refractive-index

increment was determined with a Brice-Phoenix differential refractometer was 0.220 ± 0.002 cm^3/g.

The light-scattering data were analyzed by the dissymmetry method (*22*), assuming the polymer molecules in solution could be described as polydisperse random coils, and by the Zimm-plot method (*23*). The experimental error in $\bar{M}_w$ was on the order of ± 5 to $\pm 10\%$. A more detailed report on the light-scattering measurements in TFE will be published later (*24*).

USE OF THE HYDRODYNAMIC VOLUME CONCEPT IN THE GENERATION OF MOLECULAR WEIGHT CALIBRATION CURVES

Benoit et al. (*25, 26*) and LePage, Beau, and DeVries (*27*) have shown that narrow MWD fractions of a variety of polymer types (PMMA, PS, PVC, as well as branched polymers and graft copolymers), which ordinarily have distinct molecular weight-elution volume calibration curves, have a common calibration curve when $\{[\eta]\ \bar{M}_w\}$, the effective HDV, is plotted against elution volume in THF. Similar solution behavior has been observed by other workers for linear and branched polyethylene and linear polystyrene in trichlorobenzene (*28, 29*) and in *o*-dichlorobenzene (*30*). Two methods will be discussed below whereby the HDV concept can be used to generate molecular weight calibration curves for a variety of polymer types.

Method I. Mark-Houwink Parameters Supplied

When the relationship between the intrinsic viscosity and molecular weight can be described adequately over the molecular weight range of interest by the functional form of Mark-Houwink equation,

$$[\eta] = KM^{\epsilon} \tag{2}$$

the relationship between the calibration curve for the polymer of interest, $f_x(v) = \log_{10} M_x$, and the molecular weight calibration curve for the polymer standards, $f_s(v) = \log_{10} M_s$, can be expressed according to the formalism of Coll and Prusinowski (*31*) as

$$\log_{10} M_x = \left(\frac{1}{1+\epsilon_x}\right) \log_{10}\left(\frac{K_s}{K_x}\right) + \left(\frac{1+\epsilon_s}{1+\epsilon_x}\right) f_s(v) \tag{3}$$

The Mark-Houwink parameters ϵ_s, K_s and ϵ_x, K_x refer to the standard

polymer and to the polymer of interest, respectively. For the special case of a linear calibration curve (*1*),

$$f_s(v) = \log_{10} M_S = \log_{10} D_1(s) - \{D_2(s)/2.303\}v \tag{4}$$

the calibration constants for the polymer of interest, $D_1(x)$, $D_2(x)$, can be expressed, with the aid of Eqs. (3) and (4), in terms of the calibration constants for the standard polymer, $D_1(s)$ and $D_2(s)$, as

$$D_1(x) = (K_s/K_x)^{1/(1+\epsilon_x)} D_1(s)^{[(1+\epsilon_s)/(1+\epsilon_x)]} \tag{5}$$

$$D_2(s) = \left(\frac{1+\epsilon_s}{1+\epsilon_x}\right) D_2(s) \tag{6}$$

Method II. Fit for Effective Mark-Houwink Parameters

If the Mark-Houwink parameters are unknown and there is insufficient data available for the direct generation of these parameters, effective values of ϵ and K can be obtained provided at least two out of the three experimental observables $\bar{M}_n$, $\bar{M}_w$, and $[\eta]$ are known for the polymer sample of interest. Pickett, Cantow, and Johnson (*12*) have obtained expressions for $\bar{M}_n$, $\bar{M}_w$, and $[\eta]$ in terms of the differential molecular weight distribution (DMWD) function da/dM as follows:

$$\bar{M}_n = \left[\int_{M_L}^{M_H} \frac{1}{M}\left(\frac{da}{dM}\right) dM\right]^{-1} \tag{7}$$

$$\bar{M}_w = \int_{M_L}^{M_H} M\left(\frac{da}{dM}\right) dM \tag{8}$$

$$[\eta] = K\int_{M_L}^{M_H} M^{\epsilon}\left(\frac{da}{dM}\right) dM \tag{9}$$

where

$$\frac{da}{dM} = F(v_M)\frac{1}{\left(\frac{df}{dv}\right)_{v_M}}\frac{\log_{10} e}{M} \tag{10}$$

The limits of integration M_L and M_H correspond to the lowest and highest molecular weight species, respectively, in the sample. The parameter a in the DMWD function is the weight fraction of polymer having molecular weights between M_L and M. The first factor on the right of Eq. (10), $F(v_M)$, is the normalized (i.e., area of the chromatogram is unity) baseline-adjusted chromatogram height at elution

volume v_M, and the second factor is the reciprocal of the slope of the molecular weight calibration curve at v_M. The HDV can be expressed as

$$Z = \{[\eta]M\} = KM^{\epsilon+1} \tag{11}$$

and substituted into Eqs. (7), (8), (9), and (10) to yield the expressions

$$\bar{M}_n = \left[\int_{Z_L}^{Z_H} \left(\frac{Z}{K}\right)^{-1/(\epsilon+1)} \left(\frac{da}{dZ}\right) dZ\right]^{-1} \tag{12}$$

$$\bar{M}_w = \int_{Z_L}^{Z_H} \left(\frac{Z}{K}\right)^{1/(\epsilon+1)} \left(\frac{da}{dZ}\right) dZ \tag{13}$$

$$[\eta] = K \int_{Z_L}^{Z_H} \left(\frac{Z}{K}\right)^{\epsilon/(\epsilon+1)} \left(\frac{da}{dZ}\right) dZ \tag{14}$$

$$\frac{da}{dZ} = F(v_Z) \frac{1}{\left(\frac{df_H}{dv}\right)_{v_Z}} \frac{\log_{10} e}{Z} \tag{15}$$

where now the HDV calibration curve is expressed as $f_H(v) = \log_{10} Z$. The limits of integration Z_L and Z_H correspond to the lowest and highest HDV species, respectively, in the sample. The parameter a now represents the weight fraction of polymer having HDV's between Z_L and Z. By fitting to one of the parameter sets $\{\bar{M}_n, \bar{M}_w\}$ or $\{\bar{M}_n, [\eta]\}$ in a least square sense (*32*, *33*), effective values of ϵ_x and K_x can be obtained. Then, the effective molecular weight calibration curve can be obtained from Eq. (3) or from Eqs. (4), (5), and (6) if the calibration curve is linear.

The values of ϵ_x and K_x obtained in this manner are called effective values because these parameters include the effects of (a) instrument spreading (*1*, *2*) on the chromatogram due to axial dispersion, skewing, and flattening; (b) experimental errors in $\bar{M}_n$, $\bar{M}_w$, $[\eta]$, and in the chromatogram baseline; and (c) uncertainties associated with the degree to which the polymer of interest and polymer standard lie on a common HDV calibration curve. When experimental errors and instrument spreading effects are minimized, the parameters ϵ_x and K_x should be reasonably close to the true values.

By using two to three characterized polymer samples, calibration curve segments can be obtained that span the entire elution volume range of interest. Then a smoothed calibration curve can be constructed that spans the entire elution volume range. Some smoothing

of the calibration curve segments may be necessary in the regions of overlap because of the variability in instrument spreading effects due to axial dispersion, skewing, and flattening as a function of elution volume (*1, 2*). Molecular-weight averages calculated from this smoothed curve should be closer to the absolute values than the infinite resolution values that would be obtained from a primary calibration curve of $\bar{M}_w$ vs. PEV. However, the smoothed calibration curve would retain some effects of instrument spreading at very low and very high elution volumes where the calibration curve tails up and down, respectively, due to a loss in resolution in these regions.

There are several distinct advantages of this new calibration method. It is not necessary to use very narrow MWD samples in contast to the primary calibration curve method. The entire GPC trace is used in constructing the calibration curve as opposed to one point in the primary calibration curve method. Errors associated with choosing the appropriate molecular-weight average to associate with PEV are eliminated. The measurement of $\bar{M}_w$ by light-scattering techniques is a time consuming and often experimentally difficult task and is subject to larger experimental errors than the determination of $\bar{M}_n$ by membrane or vapor pressure osmometry and $[\eta]$ by viscometry. Within the fitting technique $\bar{M}_w$ values are not required, whereas in the primary calibration curve method $\bar{M}_w$ values are needed for the construction of the $\bar{M}_w$ vs. PEV curve. As mentioned previously, instrument spreading effects are minimized by the fitting procedure. Calibration curves for both linear and branched polymers can be constructed by this method.

METHOD FOR THE GENERATION OF MOLECULAR WEIGHT AND HYDODYNAMIC VOLUME CALIBRATION CURVES IN TFE

Since the readily available well-characterized polystyrene samples are not soluble in TFE, it is not possible to construct directly a HDV calibration curve and subsequently construct molecular weight calibration curves according to Methods I and II for polymers of interest that are soluble in TFE. This difficulty can be circumvented with the aid of several samples of a given type of "test" polymer which are not necessarily narrow in MWD, but are soluble in both THF and TFE and cover the elution volume ranges of interest in both solvents.

By applying a sequence of transformations to the chromatograms of the test polymers run in THF and TFE, molecular weight and HDV calibration curves be generated in TFE. Integral distribution curves of elution volume (IDEV) for the test polymer are first constructed from the raw chromatograms. The IDEV and the wt-% polymer at elution volume v, $A(v)$, can be obtained from a transformation I on the normalized chromatogram $F(v)$ for the test polymer in THF and in TFE.

$$A_{\mathrm{THF}}(v) = I[F_{\mathrm{THF}}(v)] = -\int_{v_{M_L}}^{v} F_{\mathrm{THF}}(v)\, dv \tag{16}$$

$$A_{\mathrm{TFE}}(v) = I[F_{\mathrm{TFE}}(v)] = -\int_{v_{M_L}}^{v} F_{\mathrm{TFE}}(v)\, dv \tag{17}$$

where v_{M_L} is the elution volume in a particular solvent corresponding to the lowest molecular weight species of the sample. At equal wt-% polymer, a one-to-one correspondence can be made between the elution volume in THF, v_{THF}, and the elution volume in TFE, v_{TFE}. Thus, when

$$A_{\mathrm{THF}}(v) = A_{\mathrm{TFE}}(v) \tag{18}$$

the elution volumes in THF and TFE are related by the equations

$$v_{\mathrm{THF}} = A_{\mathrm{THF}}^{-1}\{I[F_{\mathrm{TFE}}(v)]\} \tag{19}$$

$$v_{\mathrm{TFE}} = A_{\mathrm{TFE}}^{-1}\{I[F_{\mathrm{THF}}(v)]\} \tag{20}$$

where A^{-1} is the inverse function to A.

Once the relationship between v_{THF} and v_{TFE} is established, HDV and molecular weight calibration curves in TFE can be generated from a HDV curve based on PS standards in THF. Recalling that

$$f_H(v_{\mathrm{THF}}) = \log_{10} Z \tag{21}$$

a HDV curve in TFE, g_H (v_{TFE}), can be constructed by the use of Eqs. (18), (19), (20), and (21) and is formally given by

$$g_H(v_{\mathrm{TFE}}) = \log_{10} Z = f_H[A_{\mathrm{THF}}^{-1}\{I[F_{\mathrm{TFE}}(v)]\}] \tag{22}$$

In practice the construction of the elution volume calibration (v_{THF} vs. v_{TFE}) and HDV curves in TFE is best done graphically and is illustrated in Fig. 7. By use of several samples of the test polymer the entire elution volume range of interest in both solvents can be covered. Then, molecular weight calibration curves can be constructed by Methods I and II for polymers soluble in TFE. This approach only requires that the test polymer samples be completely soluble in both

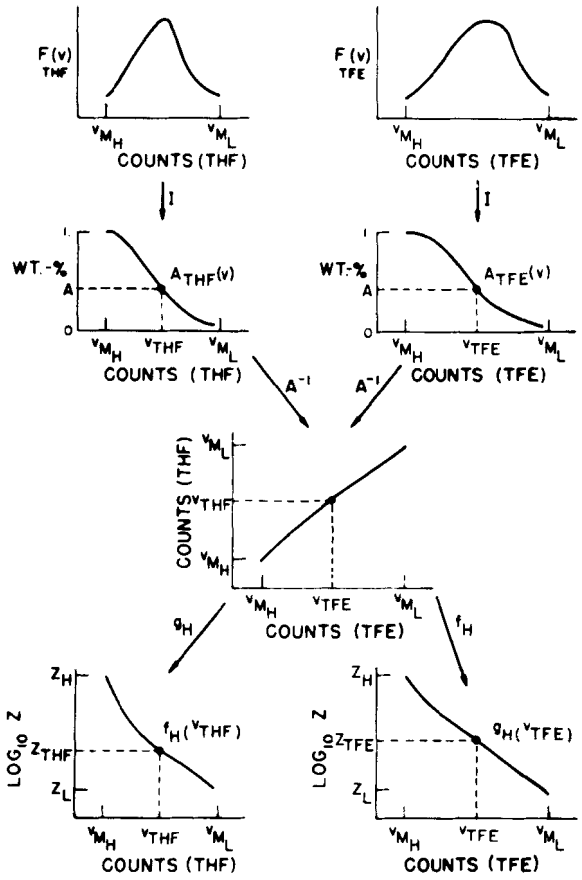

FIG. 7. Illustrative method for the generation of a hydrodynamic volume calibration curve in TFE.

solvents and that the response of the differential refractometer be linear for the sample concentrations used in both solvents.

Characterization of the test polymer samples by $\bar{M}_n$, $\bar{M}_w$, and $[\eta]$ determinations are not necessary. However, if such information is available on some of the test polymer samples, a molecular weight calibration curve can be constructed in THF by Method II. Then, a molecular weight calibration curve can be constructed in TFE through the elution volume calibration curve by the procedure discussed above. Subsequently, a HDV calibration curve can be constructed in THF if the Mark-Houwink relation for the test polymer in TFE is known.

HDV curves will be constructed for PMMA in TFE by both approaches.

RESULTS AND DISCUSSION

Generation of Molecular Weight Calibration Curves for PMMA in THF

Molecular weight calibration curves for PMMA in THF were generated by both Methods I and II and are shown in Fig. 8. The symbol $\times$ denotes the curve generated via Method I by use of Eqs. (1) and (3), Fig. 6, and the Mark-Houwink constants for PMMA in THF given in Table 3 (*3*, *4*). The calibration curve denoted by the solid line is a smoothed curve constructed from calibration curve segments for fractions D, F, and H generated by Method II. The two curves are reasonably coincident over most of the elution volume range of the fractions, diverging above 36 counts ($M < 5000$). This divergence

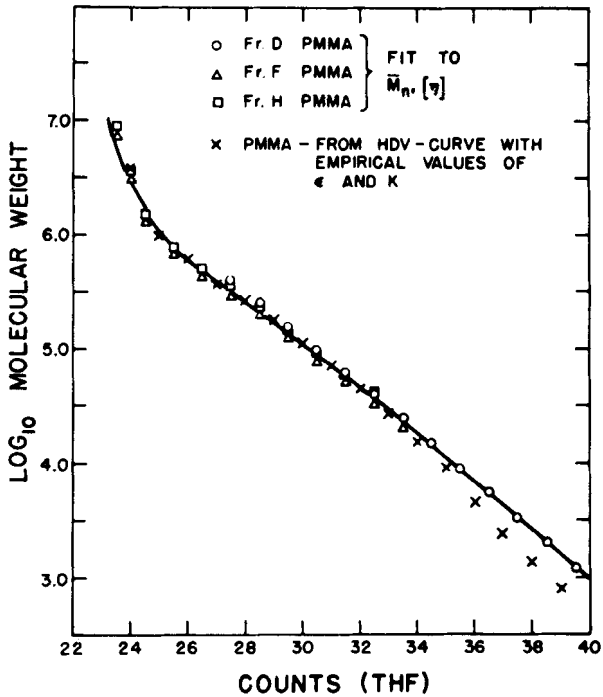

FIG. 8. PMMA molecular weight calibration curves in THF generated by Methods I and II.

can be attributed to experimental errors in the determination of $\bar{M}_n$ for fraction D and in the determination of the Mark-Houwink constants for PMMA in THF and for PS in THF for $M < 5000$. The values of $\bar{M}_n$, $\bar{M}_w$, $[\eta]$ and P calculated from these calibration curves best reflect the coincidence of the two curves. These values for fractions D, F, and H in THF are shown in Table 2 along with the corresponding true values and values obtained by directly fitting for ϵ and K. The values of $\bar{M}_n$, $\bar{M}_w$, $[\eta]$, and P calculated from these calibration curves best reflect the coincidence of the two curves. These values for fractions D, F, and H in THF are shown in Table 2 along with the corresponding true values and values obtained by directly fitting for ϵ and K. The values of $\bar{M}_n$, $\bar{M}_w$, and $[\eta]$ calculated by the various calibration procedures compare very favorably and are all closer to the true values than values normally obtained from the infinite resolution calibration curve (*1*) constructed by associating $\bar{M}_v$ or $\bar{M}_w$ with PEV. In fact, in most cases the values are within the normal experimental errors associated with the determination of $\bar{M}_n$, $\bar{M}_w$, and $[\eta]$ by membrane osmometry, light scattering, and viscometry, respectively. The larger differences in the $\bar{M}_n$, $\bar{M}_w$, $[\eta]$, and P values for fraction H are due to a loss of resolution at high molecular weights in the calibration curves of Figs. 6 and 8 characterized by a sharp upswing in the curves at very low elution volumes below 25 counts. In this region small uncertainties in the calibration curves are manifested by much larger uncertainties in the numerical calculations. Thus, over most of the elution volume range of the calibration curve above 25 counts, where good resolution by the GPC columns is attained, values of $\bar{M}_n$, $\bar{M}_w$, $[\eta]$, and P can be obtained which are in good agreement with experimental values, and do not have to be corrected for imperfect resolution due to instrument spreading effects such as dispersion, skewing, and flattening of the observer chromatogram (*1*, *2*).

The effective values of ϵ and K obtained for PMMA fraction D, F, and H in THF, by fitting to $\{\bar{M}_n, [\eta]\}$ with the aid of Eqs. (12), (14), and (15) and Fig. 6, are shown in Table 3. The effective values of ϵ and K for fraction D should lie between the corresponding set of true values, provided experimental errors and instrument spreading effects are minimal, because this fraction has molecular weights above and below the 31,000 breakpoint in the $\log_{10} [\eta]$ vs. $\log_{10} M$ curve. Similarly, the effective values of ϵ and K for fractions F and H should lie close to the corresponding true values, provided experimental errors and instrument spreading effects are minimal. The increase in ϵ and

TABLE 2

Comparison of $\bar{M}_n$, $\bar{M}_w$, $[\eta]$, and P Obtained by Several Calibration Procedures in THF and TFE for PMMA Fractions D, F, and H

Calibration Methods	$\bar{M}_n \times 10^{-3}$	$\bar{M}_w \times 10^{-3}$	$[\eta]$	P
		Fraction D		
		THF		
True value	30.8	—	0.159	—
HDV-fit to $\{\bar{M}_n, [\eta]\}$	25.2	43.8	0.180	1.73
HDV-ϵ, K supplied	31.4	53.0	0.162	1.69
Smoothed MW-curve[a]	29.7	46.2	0.186	1.56
		TFE		
True value	30.8	—	0.225	—
HDV-fit to $\{\bar{M}_n, [\eta]\}$[b]	33.1	58.6	0.239	1.77
Smoothed MW-curve[c]	23.8	44.2	0.292	1.86
		Fraction F		
		THF		
True value	130	—	0.612	—
HDV-fit to $\{\bar{M}_n, [\eta]\}$	149	213	0.522	1.43
HDV-ϵ, K supplied	126	183	0.612	1.45
Smoothed MW-curve	139	227	0.562	1.63
		TFE		
True value	130	—	1.12	—
HDV-fit to $\{\bar{M}_n, [\eta]\}$	121	184	1.10	1.53
Smoothed MW-curve	143	214	0.942	1.49
		Fraction H		
		THF		
True value	513	—	1.46	—
HDV-fit to $\{\bar{M}_n, [\eta]\}$	469	1090	1.41	2.32
HDV-ϵ, K supplied	498	1050	1.42	2.10
Smoothed MW-curve	430	873	1.22	2.03
		TFE		
True value	513	—	3.03	—
HDV-fit to $\{\bar{M}_n, [\eta]\}$	463	692	2.67	1.50
Smoothed MW-curve	490	785	2.39	1.60

[a] The smoothed MW-curve in THF refers to the calibration curve constructed from the individual calibration curves obtained from Fractions D, F, and H by fitting to $\{\bar{M}_n, [\eta]\}$ according to Method II. The smoothed MW-curve is shown in Fig. 8 as a solid line.

[b] The HDV-curve in TFE used to fit to $\{\bar{M}_n, [\eta]\}$ data refers to the calibration curve obtained by transformation of the PS–HDV–THF-curve of Fig. 6 by the v_{THF}–v_{TFE} curve of Fig. 9. This HDV curve is designated by the solid line in Fig. 10.

[c] The smoothed MW-curve in TFE refers to the calibration curve obtained by transformation of the curve described in footnote *a* by the v_{THF}–v_{TFE} curve of Fig. 9. This calibration curve is designated by the solid line in Fig. 15.

TABLE 3

Comparison of Mark-Houwink Coefficients for PMMA Fractions in THF

		ϵ	$K \times 10^4$
True value	$\bar{M}_v < 31{,}000$	0.406	21.1
	$\bar{M}_v > 31{,}000$	0.697	1.04
	HDV, fit to $\{\bar{M}_n, [\eta]\}$		
Fraction D		0.675	1.06
Fraction F		0.762	0.953
Fraction H		0.774	0.359

decrease in K with increasing molecular weight of the fractions reflect the increased effects of instrument spreading on the chromatogram due to axial dispersion, skewing, and flattening (*1*, *2*).

Construction of Hydrodynamic Volume Curves in TFE

The relationship between v_{THF} and v_{TFE} was obtained from the IDEV curves of the PMMA fractions C, D, F, G, H, I, and J in THF and in TFE according to the graphical method discussed above and illustrated in Fig. 7. A one-to-one correspondence between v_{THF} and v_{TFE} was made at the weight fractions 0.05, 0.1, 0.1, 0.3, 0.4, 0.5, 0.6, 0.7, 0.8, 0.9, and 0.95 for all the PMMA fractions. The resulting curve is shown in Fig. 9. The nonlinear regions of the curve below 25 counts (THF) and above 34 counts (THF) reflect the differences in resolving power and instrument spreading effects on the chromatogram at high and low molecular weights between the column set used with THF and the column set used with TFE.

A HDV calibration curve was constructed for TFE by using the PS-HDV curve of Fig. 6 in conjunction with the elution volume calibration curve of Fig. 9. This HDV curve is designated by the solid curve shown in Fig. 10. The construction of this curve did not require the determination of $\bar{M}_n$, $\bar{M}_w$, or $[\eta]$ for the PMMA polymer samples which are soluble in both THF and TFE. The only characterized polymer samples required were the readily available PS standards which were used for the construction of the HDV curve in THF.

For comparison purposes, a HDV curve was constructed in TFE from the smoothed PMMA molecular weight calibration curve in THF, designed at the solid line in Fig. 8, which was obtained by fitting to $\{\bar{M}_n, [\eta]\}$. This smooth PMMA–THF molecular weight calibration curve was used in conjunction with Fig. 9 to construct a

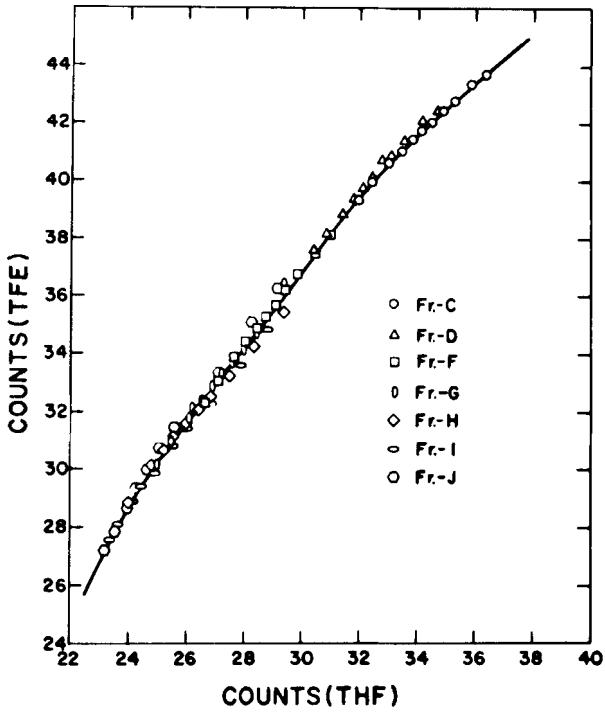

FIG. 9. Relationship between counts (THF) and counts (TFE).

PMMA molecular weight calibration curve in TFE, which is shown in Fig. 15 and designated by the solid line. Then, a HDV curve was constructed from the PMMA–TFE molecular weight calibration curve by use of Eq. (11) and the Mark-Houwink coefficients for PMMA in TFE (*34*), which are $\epsilon = 0.461$, $K = 1.81 \times 10^{-3}$ for $\bar{M}_v < 31{,}000$ and $\epsilon = 0.791$, $K = 5.95 \times 10^{-5}$ for $\bar{M}_v > 31{,}000$. This HDV curve is designated by the symbol + in Fig. 10. Within the experimental errors associated with the construction of the two HDV curves, the two curves are coincident.

Comparison of PMMA $\bar{M}_n$, $\bar{M}_w$, $[\eta]$, and P Values in TFE and in THF

The values of $\bar{M}_n$, $\bar{M}_w$, $[\eta]$, and P for the PMMA fractions D and F in THF and TFE, calculated by the various calibration procedures described in Table 2, compare favorably and agree with the corre-

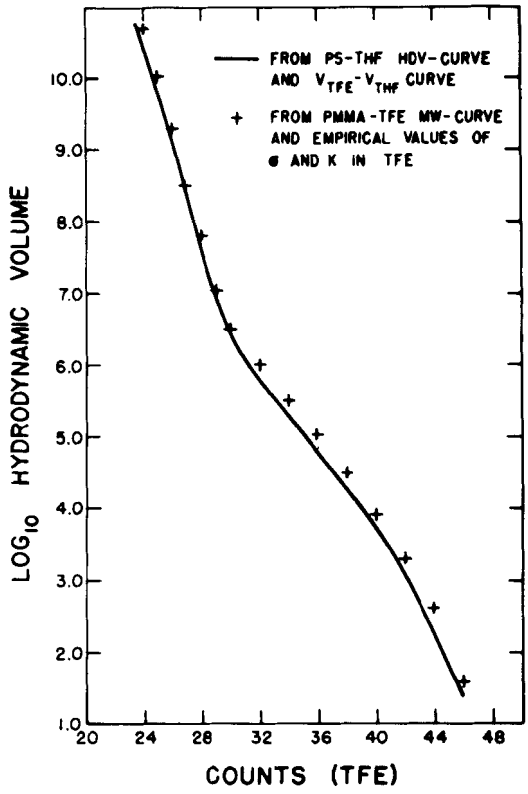

FIG. 10. Hydrodynamic volume calibration curves in TFE.

sponding true values within normal experimental errors. This is not true for fraction H. The differences in polydispersity values in THF and in TFE are too large to be attributable solely to differences in the experimental errors associated with the various procedures used to construct the calibration curves described in Table 2. The GPC columns set used with THF had nominal porosity designations, 10^6, 10^5, 10^4, 10^3, 250 Å, while the column set used with TFE had nominal porosity designations 10^7, 10^7, 10^6, 1.5×10^5, 1.5×10^4 Å. Thus, at high molecular weights the resolving power of the column set used with TFE was superior to that of the column set used with THF. Therefore, instrument spreading effects on the chromatograms run in THF were more severe than those run in TFE, resulting in much higher calculated values of $\bar{M}_w$ and consequently much higher polydispersity values.

Generation of Molecular Weight Calibration Curves for Polycaprolactams in TFE

Molecular weight calibration curves were generated for the anionically polymerized caprolactam samples and the hydrolytically polymerized caprolactam Sample P-8205, according to Method II, by using the raw chromatograms of these samples which are shown in Figs. 2–5, the HDV curve denoted by the solid line in Fig. 10, the parameter set $\{\bar{M}_n, \bar{M}_w\}$ or $\{\bar{M}_n, [\eta]\}$ for these samples, and Eqs. (3) and (7) through (10). The resulting calibration curves are shown in Figs. 11–15. No attempt was made to generate a common molecular weight calibration curve for the PC samples due to possible differences in the distribution of short- and long-chain branching in these samples (*9*, *35*). An overlay of the resulting calibration curves reveals that, indeed, there are definite molecular structural differences among

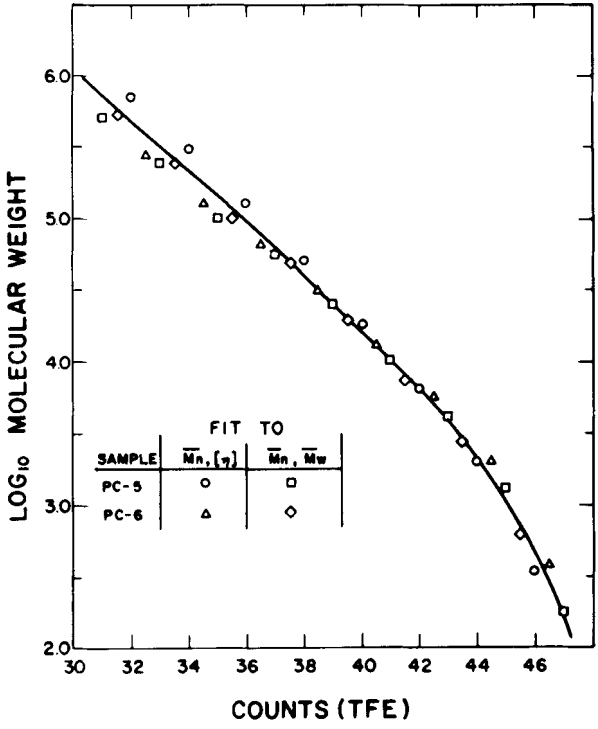

FIG. 11. Molecular weight calibration curve for Samples PC-5 and PC-6.

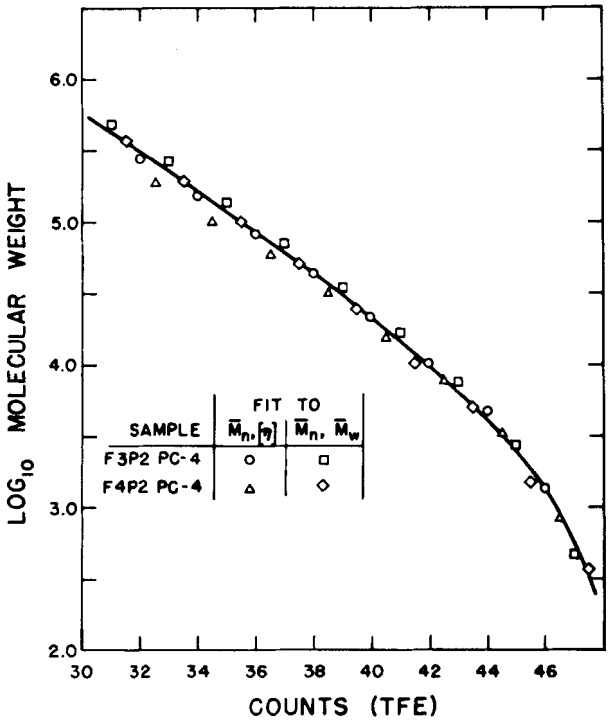

FIG. 12. Molecular weight calibration curve for Sample PC-4.

the PC samples because the curves are noncoincident. This point will be discussed further later. However, the samples were separated into classes according to the molecular weight ranges of the samples and the methods of synthesis.

Samples PC-4, PC-5, and PC-6 essentially cover the same molecular weight range. However, as shown in Table 1, PC-4 was synthesized under quite different experimental conditions than PC-5 and PC-6. In Fig. 11 a common smoothed molecular weight calibration curve was constructed from samples PC-5 and PC-6 using the calibration segments obtained for both samples by fitting separately to both parameter sets $\{\bar{M}_n, [\eta]\}$ and $\{\bar{M}_n, \bar{M}_w\}$. Over the common elution volume range of the samples, $35 < v_{\mathrm{TFE}} < 44$, the four calibration curve segments represented by symbols in Fig. 11 are coincident within experimental errors. Outside of the elution volume ranges of the samples, the calibration curve segments tend to be divergent. However,

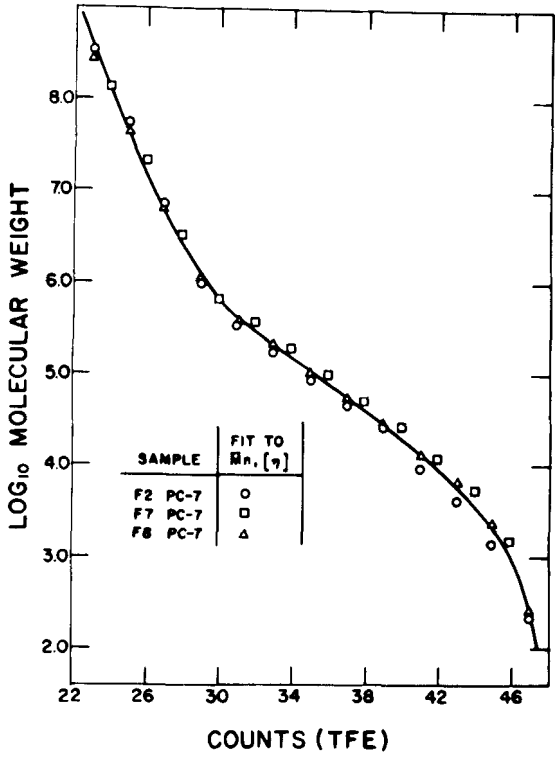

FIG. 13. Molecular weight calibration curve for Sample PC-7.

this behavior is to be expected in the extrapolated region of the count range due to the effects of experimental errors in $\bar{M}_n$, $\bar{M}_w$, $[\eta]$, and the chromatogram baseline, which are reflected in the fitted values of ϵ and K. Examination of Table 4 shows that the values of $\bar{M}_n$, $\bar{M}_w$, $[\eta]$, and P calculated by the various calibration procedures compare very favorably with the corresponding true values. The smoothed values generally do not agree as well with the true values as do the values obtained from fitting to $\{\bar{M}_n, [\eta]\}$ or to $\{\bar{M}_n, \bar{M}_w\}$. The smooth curve designated by the solid line in Fig. 11 was the result of subjective averaging by eye of the four calibration segments. A better smoothed curve would result if the data from the four calibration segments were smoothed in a least-square sense by fitting to the mathematical form of the Yau-Malone function (*32, 33, 36*). It is interesting to note that the $\bar{M}_w$ values resulting from the fit to $\{\bar{M}_n, [\eta]\}$ are in excellent agreement with the true values. Thus, the fitting

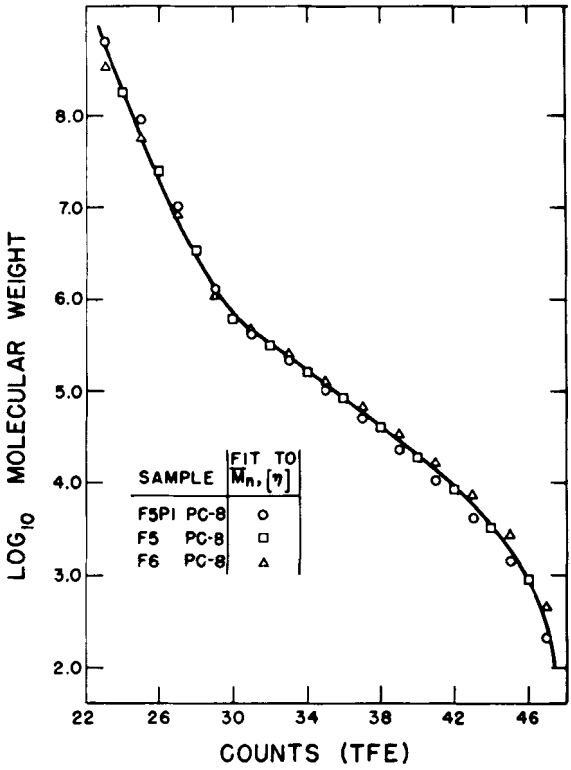

FIG. 14. Molecular weight calibration curve for Sample PC-8.

procedure via the HDV concept eliminates the necessity of empirically determining $\bar{M}_w$ values. The agreement of the calculated values of $\bar{M}_n$ and $[\eta]$, obtained from fitting to $\{\bar{M}_n, [\eta]\}$, with their respective true values; and the agreement of the calculated values of $\bar{M}_n$ and $\bar{M}_w$, obtained from fitting to the parameter set $\{\bar{M}_n, \bar{M}_w\}$, with their respective true values reflect the degree of fit obtained from the least-square process. The degree of fit reflects the experimental errors associated with $\bar{M}_n$, $\bar{M}_w$, $[\eta]$, the observed chromatogram, and the construction of the HDV curve.

Fractions F3P2 aid F4P2 of Sample PC-4 were used to construct a calibration curve for Sample PC-4. The calibration segments were generated by fitting to both parameter sets $\{\bar{M}_n, [\eta]\}$ and $\{\bar{M}_n, \bar{M}_w\}$, and are shown in Fig. 12 along with the smoothed curve designated by the solid line. The values of $\bar{M}_n$, $\bar{M}_w$, and $[\eta]$ in Table 5 calculated

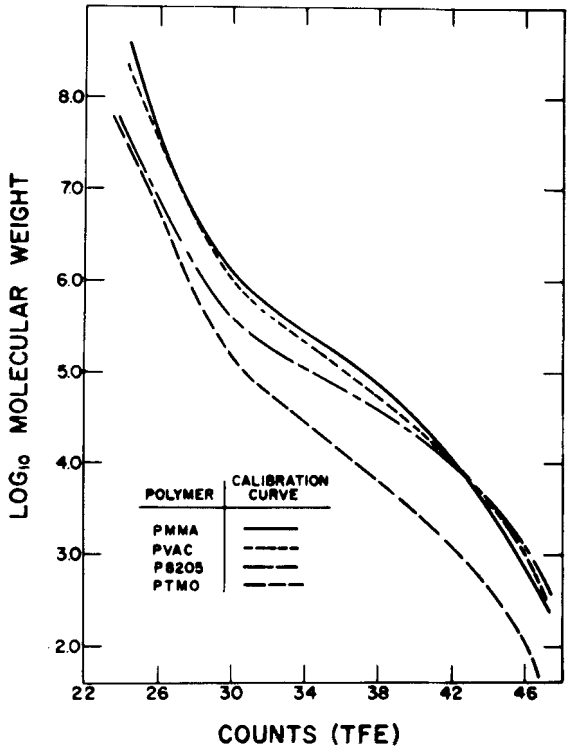

FIG. 15. Molecular weight calibration curves for PMMA, PVAC, P8205, and PTMO polymers.

by the various calibration procedures compare favorably with their respective true values. The general quality of the results is the same as that for Samples PC-5 and PC-6. When the calibration curves of Figs. 11 and 12 are overlaid, it is seen that the two curves cross at $M \approx 40{,}000$. For $M < 40{,}000$ the calibration curve of PC-5 and PC-6 lies below that of PC-4. The converse is true for $M > 40{,}000$. These differences are greater than the experimental errors associated with the construction of these calibration curves and are believed to reflect molecular structural differences associated with the branching distributions of these samples. When these calibration curves are compared to that of the hydrolytically polymerized caprolactam Sample P8205 of Fig. 15, it is seen that they lie above the P8205 curve for $M > 10{,}000$. Based on the similar results of Drott and Mendelson (*28*) and Wild and Guliana (*29*) in their GPC studies of the effects of long-chain

TABLE 4

Comparison of $\bar{M}_n$, $\bar{M}_w$, $[\eta]$, and P Obtained by Several Calibration Procedures in TFE for PC-5 and PC-6

Calibration method	$\bar{M}_n \times 10^{-3}$	$\bar{M}_w \times 10^{-3}$ [a]	$[\eta]$	P	Fitted values ϵ	Fitted values $K \times 10^3$
		PC-5				
True value	8.52	(17.7)	0.45	2.08	—	—
HDV-fit to $\{\bar{M}_n, [\eta]\}$	8.52	22.0	0.45	2.59	0.335	16.0
HDV-fit to $\{\bar{M}_n, \bar{M}_w\}$	8.52	17.7	0.52	2.08	0.573	1.96
Smoothed MW-curve[b]	8.05	15.8	(0.53)[k]	1.97	—	—
		PC-6				
True value	18.2	43.0 (35.5)	0.85	2.36 (1.95)	—	—
HDV-fit to $\{\bar{M}_n, [\eta]\}$	18.8	38.3	0.89	2.03	0.635	1.05
HDV-fit to $\{\bar{M}_n, \bar{M}_w\}$[c]	18.2	39.2	0.86	2.15	0.445	7.32
Smoothed MW-Curve[b]	22.3	34.7	(0.88)[d]	1.55	—	—

[a] The true $\bar{M}_w$ values enclosed in parenthesis were determined by the dissymmetry method while those not enclosed in parenthesis were determined by the Zimm-plot method.

[b] The smoothed MW-curve was constructed from calibration curves for the samples generated by fitting to $\{\bar{M}_n, [\eta]\}$ and $\{\bar{M}_n, \bar{M}_w\}$ using the HDV-curve denoted by a solid line in Fig. 10.

[c] The average of the dissymmetry method and Zimm-plot method values of $\bar{M}_w$ was used in fitting to $\{\bar{M}_n, \bar{M}_w\}$.

[d] The values of $[\eta]$ in parenthesis were those determined using Mark-Houwink coefficients for linear PC in TFE. These coefficients were determined using experimental data on samples of PC, $[\eta]^{50}_{\text{TFE}}$, $[\eta]^{25°}_{m\text{-cresol}}$, and literature values (*37*) of Mark-Houwink coefficients for linear PC in *m*-cresol-at 25°C. This work will be published later (*10*).

branching in polyethylene, it can be concluded that the hydrolytically polymerized P8205 sample is much more linear than the anionically polymerized PC-4, PC-5, and PC-6 samples.

The calibration curves constructed from Fractions F2, F7, and F8 of Sample PC-7 and Fractions F5P1, F5, and F6 of Sample PC-8 are shown in Figs. 13 and 14, respectively. The calculated values of $\bar{M}_n$, $\bar{M}_w$, $[\eta]$, and P for the fractions of Samples PC-7 and PC-8, ob-

TABLE 5

Comparison of $\bar{M}_n$, $\bar{M}_w$, $[\eta]$, and P Obtained by Several Calibration Procedures in TFE for Fractions of PC-4

Calibration method	$\bar{M}_n \times 10^{-3}$	$\bar{M}_w \times 10^{-3}$ [a]	$[\eta]$	P	Fitted values ϵ	Fitted values $K \times 10^3$
		F3P2 PC-4				
True value	31.5	60.5 (61.0)	1.15	1.92 (1.94)	—	—
HDV-fit to $\{\bar{M}_n, [\eta]\}$	23.6	59.8	0.90	2.54	0.906	0.0423
HDV-fit to $\{\bar{M}_n, \bar{M}_w\}$ [b]	25.1	69.2	0.78	2.75	0.801	0.103
Smoothed MW-curve [c]	22.9	51.3	(1.14) [k]	2.24	—	—
		F4P2 PC-4				
True value	23.2	67.0 (62.0)	1.33	2.89 (2.67)	—	—
HDV-fit to $\{\bar{M}_n, [\eta]\}$	21.7	52.8	1.25	2.44	0.980	0.0294
HDV-fit to $\{\bar{M}_n, \bar{M}_w\}$ [b]	23.2	67.0	0.99	2.89	0.772	0.188
Smoothed MW-curve [c]	24.9	60.3	(1.28) [d]	2.43	—	—

[a] The true $\bar{M}_w$ values enclosed in parenthesis were determined by the dissymmetry method while those not enclosed in parenthesis were determined by the Zimm-plot method.

[b] The smoothed MW-curve was constructed from calibration curves for the samples generated by fitting to $\{\bar{M}_n, [\eta]\}$ and $\{\bar{M}_n, \bar{M}_w\}$ using the HDV-curve denoted by a solid line in Fig. 10.

[c] The average of the dissymmetry method and Zimm-plot method values of $\bar{M}_w$ was used in fitting to $\{\bar{M}_n, \bar{M}_w\}$.

[d] The values of $[\eta]$ in parenthesis were those determined using Mark-Houwink coefficients for linear PC in TFE. These coefficients were determined using experimental data on samples of PC, $[\eta]^{50}_{\text{TFE}}$, $[\eta]^{25°}_{m\text{-cresol}}$, and literature values (*37*) of Mark-Houwink coefficients for linear PC in *m*-cresol-at 25°C. This work will be published later (*10*).

tained by fitting to $\{\bar{M}_n, [\eta]\}$ and obtained by using the smoothed calibration curves of Figs. 13 and 14, are shown in Tables 6 and 7, respectively, along with the true values of $\bar{M}_n$ and $[\eta]$. The general quality of the graphical and calculated results are similar to that obtained for Samples PC-4, PC-5, and PC-6. Upon overlaying the calibration curves for Samples PC-7, PC-8, and P8205, it is seen that the calibration curve for PC-7 lies above that for P8205 and the calibra-

TABLE 6

Comparison of $\bar{M}_n$, $\bar{M}_w$, $[\eta]$, and P Obtained by Several Calibration Procedures in TFE for Fractions of PC-7

Calibration method	$\bar{M}_n \times 10^{-3}$	$\bar{M}_w \times 10^{-3}$	$[\eta]$	P	Fitted values ϵ	Fitted values $K \times 10^3$
		F2 PC-7				
True value	7.69	—	1.04	—	—	—
HDV-fit to $\{\bar{M}_n, [\eta]\}$	7.69	35.2	1.04	4.58	0.703	0.725
Smoothed MW-curve[a]	10.7	45.6	(1.03)[b]	4.27	—	—
		F7 PC-7				
True value	165	—	5.97	—	—	—
HDV-fit to $\{\bar{M}_n, [\eta]\}$	166	1000	5.95	6.09	0.856	0.0502
Smoothed MW-curve[a]	118	769	(7.32)[b]	6.50	—	—
		F8 PC-7				
True value	140	—	5.29	—	—	—
HDV-fit to $\{\bar{M}_n, [\eta]\}$	140	563	5.30	4.03	0.831	0.105
Smoothed MW-curve[a]	132	540	(5.62)[b]	4.09	—	—

[a] The smoothed MW-curve was constructed from calibration curves generated for the samples in the Table by fitting to $\{\bar{M}_n, [\eta]\}$ using the HDV curve denoted by the solid line in Fig. 10.

[b] The values of $[\eta]$ in parenthesis were those determined using Mark-Houwink coefficients for linear PC in TFE. These coefficients were determined using experimental data on samples of PC, $[\eta]^{50}_{\text{TFE}}$, $[\eta]^{25^\circ}_{m\text{-cresol}}$, and literature values (*37*) of Mark-Houwink coefficients for linear PC in *m*-cresol-at 25°C. This work will be published later (*10*).

tion curve for PC-8 lies above that of PC-7 and P-8205. This would indicate that PC-8 is more branched than PC-7 and that Samples PC-7 and PC-8 are considerably more branched than Sample P8205.

Branching in Samples PC-7 and PC-8 also is reflected in the values of $[\eta](l)$, the intrinsic viscosity of a linear polymer having the same DMWD as the polymer in question, which may be branched. The values of $[\eta](l)$ for the fractions of PC-7 and PC-8 are computed from Eq. (9) using the Mark-Houwink coefficients for linear PC in TFE. These coefficients were obtained as described in footnote *d* in Table 4 and are $\epsilon = 0.736$ $K = 5.11 \times 10^{-4}$ for $\bar{M}_v > 29{,}000$. This work will be published later (*10*). The values of $[\eta](l)$ for fractions of PC-7 and PC-8 are shown in Tables 6 and 7, respectively, and designated by the superscript k. The DMWD function, da/dM, used

TABLE 7

Comparison of $\bar{M}_n$, $\bar{M}_w$, $[\eta]$, and P Obtained by Several Calibration Procedures in TFE for Fractions of PC-8

Calibration method	$\bar{M}_n \times 10^{-3}$	$\bar{M}_w \times 10^{-3}$	$[\eta]$	P	Fitted values	
					ϵ	$K \times 10^3$
		F5P1 PC-8				
True value	118	—	4.73	—	—	—
HDV-fit to $\{\bar{M}_n, [\eta]\}$	118	926	4.75	7.87	0.632	1.12
Smoothed MW-curve[a]	142	713	(6.75)[b]	5.01	—	—
		F5 PC-8				
True value	202	—	7.41	—	—	—
HDV-fit to $\{\bar{M}_n, [\eta]\}$	202	1290	7.42	6.38	0.728	0.332
Smoothed MW-curve[a]	209	1080	(9.50)[b]	5.18	—	—
		F6 PC-8				
True value	183	—	6.79	—	—	—
HDV-fit to $\{\bar{M}_n, [\eta]\}$	183	1160	6.79	6.34	0.819	0.0865
Smoothed MW-curve[a]	155	994	(8.82)[b]	6.42	—	—

[a] The smoothed MW-curve was constructed from calibration curves generated for the samples in the Table by fitting to $\{\bar{M}_n, [\eta]\}$ using the HDV curve denoted by the solid line in Fig. 10.

[b] The values of $[\eta]$ in parenthesis were those determined using Mark-Houwink coefficients for linear PC in TFE. These coefficients were determined using experimental data on samples of PC, $[\eta]^{30}_{\text{TFE}}$, $[\eta]^{25^\circ}_{m\text{-cresol}}$, and literature values (*37*) of Mark-Houwink coefficients for linear PC in *m*-cresol-at 25°C. This work will be published later (*10*).

in Eq. (9) is given by Eq. (10), where now $f(v) = \log_{10} M$ is the smoothed molecular weight calibration curves for Samples PC-7 and PC-8 shown in Figs. 13 and 14, respectively.

If the polymer in question is linear, the values of $[\eta](l)$ calculated in this manner will agree with the experimental value, $[\eta](t)$, within reasonable experimental errors. If the polymer in question is branched, then $[\eta](t) < [\eta](l)$. Therefore, the ratio $[\eta](t)/[\eta](l) = g^b$, which shall be designated as the branching factor, is a measure of the degree of long-chain branching in the sample. The parameter g is the classical branching index which is related to the weight-average number of branch points per molecule, n_w (*38*, *39*) and depends upon the type of branching (i.e., random, comb, or star-type). The value of the parameter b depends upon the type of branching and usually lies in the

range $\frac{1}{2} \leq b \leq \frac{3}{2}$ (*38*). It is important to note that the branching factor calculated by the above method is a ratio of intrinsic viscosities of a linear and branched polymer having the same DMWD curve (i.e., the same $\bar{M}_n$, $\bar{M}_w$, $\bar{M}_z$, $\bar{M}_{z+1}$, etc.). Since the branched calibration curve has molecular weight greater than or equal to the linear calibration curve at corresponding elution volumes, the chromatogram of the linear polymer having the same DMWD as the branched polymer would have elution volumes less than or equal to that of the branched polymer at corresponding molecular weights. Thus the chromatograms of the linear and branched polymer having the same DMWD would be distinct.

This approach suggests a means of generating g^b values as a function of molecular weight for the linear and branched polymer having the same DMWD, independent of a specific molecular branching model relating g to n_w, by using characterized narrow MWD fractions of the branched polymer. Previous approaches have resorted to specific branching models and used g^b values where $[\eta](l)$ was calculated at the same $\bar{M}_w$ or $\bar{M}_v$ value as the branched polymer and not at the same DMWD. If only $\bar{M}_n$ and $[\eta]$ are readily available for these fractions, $\bar{M}_w$ values can be calculated for each fraction from the generated segmental calibration curve. Subsequently the $[\eta]$–$\bar{M}_w$ and g^b behavior can be obtained over the entire molecular weight range.

The value of $[\eta](l)$ obtained in this manner for F2 PC-7 is in good agreement with the true value indicating that this fraction has negligible amounts of long-chain branching that is detectable by intrinsic viscosity measurements. This is not unexpected because of the low molecular weights of this fraction. However, F7 PC-7 and F8 PC-7 have $[\eta](l)$ values greater than the true values indicating that these fractions, indeed, do have significant amounts of long-chain branching. Similarly, comparison of $[\eta](l)$ values for Fractions F5P1, F5, and F6 of Sample PC-8 with the corresponding true values shows these fractions to contain significant amounts of long-chain branching. The values of the branching factor g^b for the Fractions F7 PC-7 and F8 PC-7 are 0.82 and 0.94, respectively, while the values of g^b for the fractions F5P1 PC-8, F5 PC-8, and F6 PC-8 are 0.70, 0.78, and 0.77, respectively. Upon taking into consideration the large polydispersities of these fractions and the experimental errors contributing to the values of $[\eta](l)$, it can be seen that at high molecular weights Sample PC-8 has a greater degree of long-chain branching than does Sample PC-7. The results of this analysis are in qualitative accord

with the earlier observation that Sample PC-8 should have a greater degree of long-chain branching than Sample PC-7 because of the nature of the molecular weight calibration curves.

Generation of Molecular Weight Calibration Curves for PVAC and PTMO

Molecular weight calibration curves for PVAC and PTMO were generated in TFE by fitting to the parameter sets $\{\bar{M}_n, [\eta]\}$ and

TABLE 8

Comparison of $\bar{M}_n$, $\bar{M}_w$, $[\eta]$, and P Obtained by Several Calibration Procedures in THF for PVAC, P8205, and PTMO

Calibration method	$\bar{M}_n \times 10^{-3}$	$\bar{M}_w \times 10^{-3}$	$[\eta]$	P	Fitted values ϵ	Fitted values $K \times 10^3$
		PVAC				
True value	58.6	—	1.40	—	—	—
HDV-fit to $\{\bar{M}_n, [\eta]\}$	58.4	223	1.40	3.81	0.681	0.380
		P8205				
True value	25.4	—	1.87	—	—	—
HDV-fit to $\{\bar{M}_n, [\eta]\}$	23.3	68.2	1.73	2.92	1.02	0.0199
		PTMO				
True value	107	800[a]	—	7.47	—	—
HDV-fit to $\{\bar{M}_n, \bar{M}_w\}$	107	799	—	7.47	0.643	16.3

[a] The $\bar{M}_w$ value was supplied by Dr. R. E. Wetton.

$\{\bar{M}_n, \bar{M}_w\}$, respectively; and using the raw chromatograms of these samples which are shown in Fig. 5, the HDV curve designated by the solid line in Fig. 10, and Eqs. (3) and (7) through (10). The calibration curves are shown in Fig. 15. The calculated values of $\bar{M}_n$, $\bar{M}_w$, and $[\eta]$ are shown in Table 8 and agree with the respective true values well within the usual experimental errors. Figure 15 is a composite plot of the molecular weight calibration curves for the linear polymers PMMA, PVAC, P8205, and PTMO. All but PTMO tend to coalesce to a common point at $M \approx 6000$. The divergence of the curves below this point probably is due to the effect of experimental errors on the numerical calculations in the construction of these curves. The divergence of the curves above this point reflects differences in the effective hydrodynamic molecular volumes among these polymer types. The molecular weight calibration curve for PTMO lies well below the

curves for PMMA, PVAC, and P8205. From Fig. 5 it can be seen that the elution volumes of the PTMO sample cover the range $24.2 < v_{TFE} < 36.5$. The extrapolated curve above 36.5 counts, based on the fitted ϵ and K values, reflects experimental errors and instrument spreading effects on the chromatogram of this sample. At high molecular weights (low elution volumes) chromatogram spreading as measured by skewing, dispersion, and flattening parameters (*1*, *2*) will significantly effect the magnitude of the fitted values of ϵ and K. Therefore, the use of these values to extrapolate the calibration curve to lower molecular weights may lead to an unrealistic calibration curve in this region.

CONCLUSIONS

The HDV concept has been used to generate molecular weight calibration curves by (I) using empirical Mark-Houwink parameters and (II) generating effective Mark-Houwink parameters by fitting to the parameter set $\{\bar{M}_n, \bar{M}_w\}$ or $\{\bar{M}_n, [\eta]\}$. Molecular weight calibration curves generated by these methods for PMMA in THF were shown to be coincident over the elution volume range of the samples, within experimental errors. This coincidence was reflected in a comparison of the calculated values of $\bar{M}_n$ and $[\eta]$ with the corresponding true values.

Some of the advantages in using Method II for the generation of molecular weight calibration curves are as follows:

(a) Only two to three characterized samples, which can have broad MWD's, are needed for the construction of the calibration curve to cover a wide elution volume range.
(b) The entire GPC trace of the sample is used in constructing the calibration curve as opposed to one point in the primary calibration curve method.
(c) Instrument spreading effects are minimized by the fitting procedure.
(d) By fitting to $\{\bar{M}_n, [\eta]\}$, the necessity for the measurement of $\bar{M}_w$ by light-scattering techniques is eliminated because $\bar{M}_w$ can be obtained from the generated calibration curve.

A method has been presented for the generation of a HDV calibration curve in TFE from which molecular weight calibration curves can be generated by Method II for a variety of polymers. This method

makes use of the HDV curve in THF, generated from the readily available PS standards.

REFERENCES

1. T. Provder and E. M. Rosen, *Separ. Sci.*, **5**, 437 (1970).
2. E. M. Rosen and T. Provder, *Separ. Sci.*, **5**, 485 (1970).
3. C. V. Goebel, "Fourth International GPC Seminar," Miami Beach, Florida, Seminar Proceedings, 90 (1967).
4. J. D. Gouveia, L. A. Prince, and H. E. Staplefeldt, "Sixth International GPC Seminar," Miami Beach, Florida, Seminar Proceedings, 78 (1968).
5. W. A. Dark, R. F. Levangie, and K. S. Bombaugh, *Ibid.*, p. 414.
6. T. G Fox, J. B. Kinsingner, H. F. Mason, and E. M. Schuele, *Polymer*, **3**, 71 (1962).
7. T. Provder, J. H. Clark, and E. E. Drott, Unpublished Data.
8. G. B. Gechele and G. Stea, *Eur. Polym. J.*, **1**, 91 (1965).
9. R. Z. Greenley, J. C. Stauffer, and J. E. Kurz, *Macromolecules*, **2**, 561 (1969).
10. T. Provder, M. Ohta, and J. C. Woodbrey, Unpublished Data.
11. W. W. Yau, H. L. Suchan, and C. P. Malone, *J. Polym. Sci., Part A-2*, **6**, 1349 (1968).
12. H. E. Pickett, M. J. R. Cantow, and J. F. Johnson, *J. Appl. Polym. Sci.*, **10**, 917 (1966).
13. D. F. Alliet and J. M. Pacco, "Sixth International GPC Seminar," Miami Beach, Florida, Seminar Proceedings, 274 (1968).
14. ArRo Laboratories, Inc., *Membranes for Osmometry, Conditioning Procedures for Organic Solvents*, 1967.
15. W. R. Krigbaum and P. J. Flory, *J. Polym. Sci.*, **9**, 503 (1952).
16. F. Daniels, J. W. Williams, P. Bender, R. A. Alberty, and C. D. Cornwell, *Experimental Physical Chemistry*, McGraw-Hill, New York, 1962, p. 452.
17. J. Brandrup and E. H. Immergut, *Polymer Handbook*, Wiley (Interscience), New York, 1966, p. VIII-53.
18. G. V. Schulz and E. Blaschke, *J. Prakt. Chem.*, **158**, 130 (1941).
19. W. Heller, *J. Colloid Sci.*, **9**, 547 (1954).
20. F. W. Ibrahim, *J. Polym. Sci., Part A*, **3**, 469 (1965).
21. J. E. Kurz, *J. Polym. Sci., Part A*, **3**, 1895 (1965).
22. P. J. Debye, *J. Phys. Colloid Chem.*, **51**, 18 (1947).
23. B. H. Zimm, *J. Chem. Phys.*, **16**, 1093 (1948).
24. M. Ohta, T. Provder, and J. C. Woodbrey, Unpublished Data.
25. H. Benoit, Z. Grubisic, P. Rempp, D. Decker, and J. G. Zilliox, *J. Chem. Phys.*, **63**, 1507 (1966).
26. M. Benoit, Z. Grubisic, and P. Rempp, *J. Polym. Sci., Part B*, **5**, 753 (1967).
27. M. LePage, R. Beau, and A. J. DeVries, *J. Polym. Sci., Part C*, **21**, 119 (1968).
28. E. E. Drott and R. A. Mendelson, "Fifth International GPC Seminar," London, England, Seminar Proceedings, No. 15 (1968).
29. L. Wild and R. Guliana, *J. Polym. Sci., Part A-2*, **5**, 1087 (1967).
30. D. J. Pollock and R. F. Kratz, "Sixth International GPC Seminar," Miami Beach, Florida, Seminar Proceedings, 336 (1968).

31. H. Coll and L. R. Prusinowski, *J. Polym. Sci., Part B,* **5,** 1153 (1967).
32. D. W. Marquardt, *J. Soc. Ind. Appl. Math.,* **2,** 431 (1963).
33. E. J. Henley and E. M. Rosen, *Material and Energy Balance Computations,* Wiley, New York, 1969, p. 547f and pp. 560–566.
34. T. Provder, J. C. Woodbrey, and J. H. Clark, Unpublished Data.
35. O. Wichterle, J. Šebenda, and J. Káliček, *Fortschr. Hochpolym. Forsch.,* **2,** 578 (1961).
36. W. W. Yau and C. P. Malone, *J. Polym. Sci., Part B,* **5,** 663 (1967).
37. Z. Tuzar, P. Kratochvil, and M. Bohdanecky, *J. Polym. Sci., Part C,* **16,** 663 (1967).
38. M. L. Miller, *The Structure of Polymers,* Reinhold, New York, 1966, pp. 124–131.
39. R. A. Mendelson and E. E. Drott, *J. Polym. Sci., Part B,* **6,** 795 (1968).

Received by editor March 17, 1970